

Supporting Information for

**Fertilization-driven Pulses of Atmospheric Nitrogen Dioxide Complicate Air Pollution  
in Early Spring over North China**

Tian Feng,<sup>1</sup> Guohui Li,<sup>2,\*</sup> Shuyu Zhao,<sup>3</sup> Naifang Bei,<sup>4</sup> Xin Long,<sup>5</sup> Yuepeng Pan,<sup>6</sup> Yu Song,<sup>7</sup> Ruonan Wang,<sup>2</sup> Xuexi Tie,<sup>2</sup> Luisa T. Molina<sup>8</sup>

<sup>1</sup> Department of Geography & Spatial Information Techniques, Ningbo University, Ningbo, China

<sup>2</sup> KLACP, State Key Laboratory of Loess and Quaternary Geology, Institute of Earth Environment, Chinese Academy of Sciences, Xi'an, China

<sup>3</sup> Ningbo Meteorological Bureau, Ningbo, China

<sup>4</sup> School of Human Settlements and Civil Engineering, Xi'an Jiaotong University, Xi'an, China

<sup>5</sup> Research Center for Atmospheric Environment, Chongqing Institute of Green and Intelligent Technology, Chinese Academy of Sciences, Chongqing, China

<sup>6</sup> State Key Laboratory of Atmospheric Boundary Layer Physics and Atmospheric Chemistry (LAPC), Institute of Atmospheric Physics, Chinese Academy of Sciences, Beijing, China

<sup>7</sup> State Key Joint Laboratory of Environmental Simulation and Pollution Control, Department of Environmental Science, Peking University, Beijing, China

<sup>8</sup> Molina Center for Energy and the Environment, La Jolla, CA, USA

\* Corresponding author. Email: [ligh@ieecas.cn](mailto:ligh@ieecas.cn)

**The PDF file includes:**

Texts S1-S2

Figures S1 to S4

References

### **Text S1. Definition of pollution accumulation index (PAI)**

Boundary layer height (BLH) and wind speed (WS) are crucial meteorological fields for the occurrence of air pollutions, reflecting the atmospheric circulation conditions directly (Huang et al., 2017; Korshover and Angell, 2000; Su et al., 2018). Here, a pollution accumulation index (PAI) is defined using BLH (km) and WS ( $\text{m s}^{-1}$ ) to represent the atmospheric dispersion capacity. The formula is as follows:

$$PAI = \frac{I}{BLH} \times \frac{I}{e^{WS}} \quad (4)$$

where PAI is dimensionless. The higher (lower) the PAI is, the poorer (better) the ventilation is and the more (less) the pollutants accumulate. The data are freely from the ERA5 products by the European Centre for Medium-Range Weather Forecasts. A higher PAI generally indicates meteorology being more favorable for pollution accumulation.

### **Text S2. Evaluation indices for simulation vs. observation**

Three statistical indices, including mean bias (MB), normalized mean bias (NMB), root mean square error (RMSE), and index of agreement (IOA), are used to evaluate the model performance on mass concentrations of surface pollutants (Feng et al., 2021; Willmott, 1981):

$$IOA = 1 - \frac{\sum_{i=1}^N (S_i - O_i)^2}{\sum_{i=1}^N (|S_i - \bar{O}| + |O_i - \bar{O}|)^2} \quad (5)$$

$$MB = \frac{1}{N} \sum_{i=1}^N (S_i - O_i) \quad (6)$$

$$NMB = \frac{\sum_{i=1}^N (S_i - O_i)}{\sum_{i=1}^N O_i} \times 100\% \quad (7)$$

$$RMSE = \left[ \frac{1}{N} \sum_{i=1}^N (S_i - O_i)^2 \right]^{\frac{1}{2}} \quad (8)$$

where  $S_i$  and  $O_i$  are the simulated and observed variables, respectively.  $N$  is the total number of simulation variables, and  $\bar{O}$  denotes the average of observations. The IOA varies in the range from 0 to 1, and higher values suggest better agreement between the simulation and the observation.

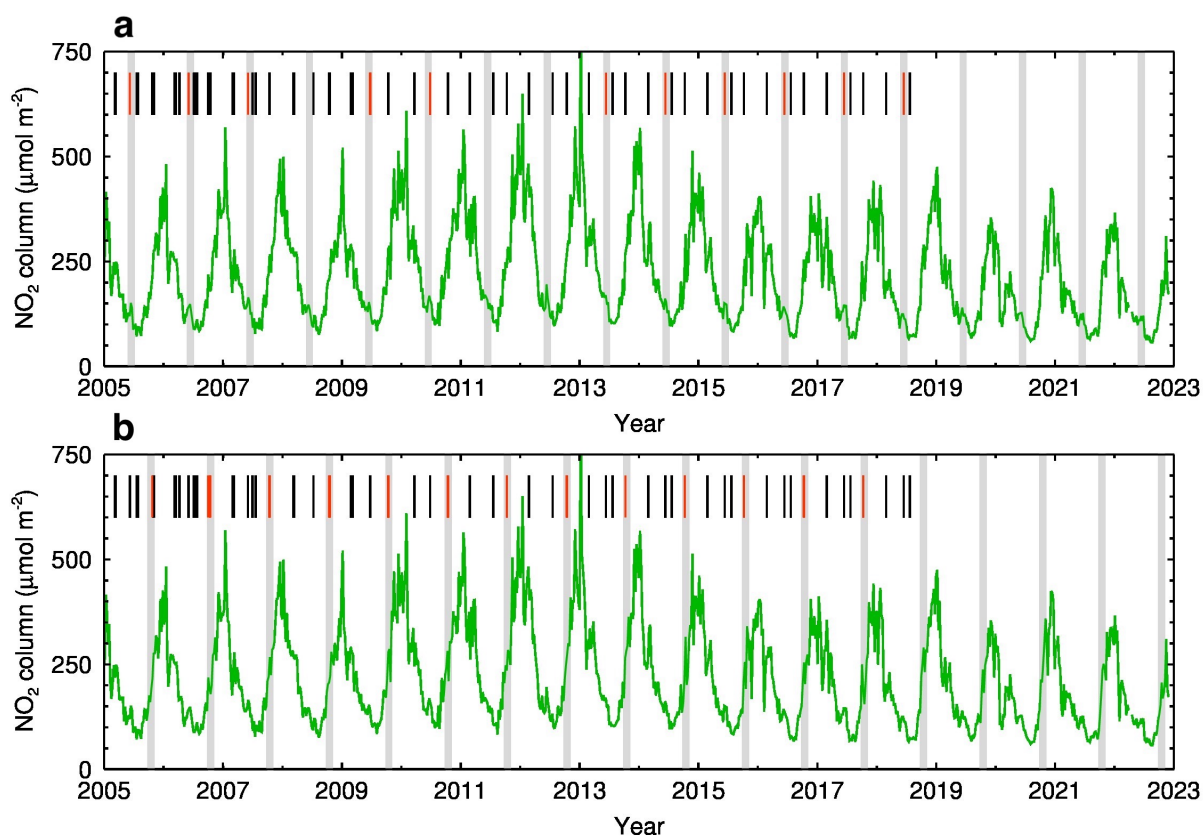


**Figure S1.** Other sub-peaks of NO<sub>2</sub> column. (a and b) Satellite-derived other pulses of NO<sub>2</sub> column in June and October, respectively. Intersections of the gray bars and the green lines, and the short bars are similar to those in Figure 1a.

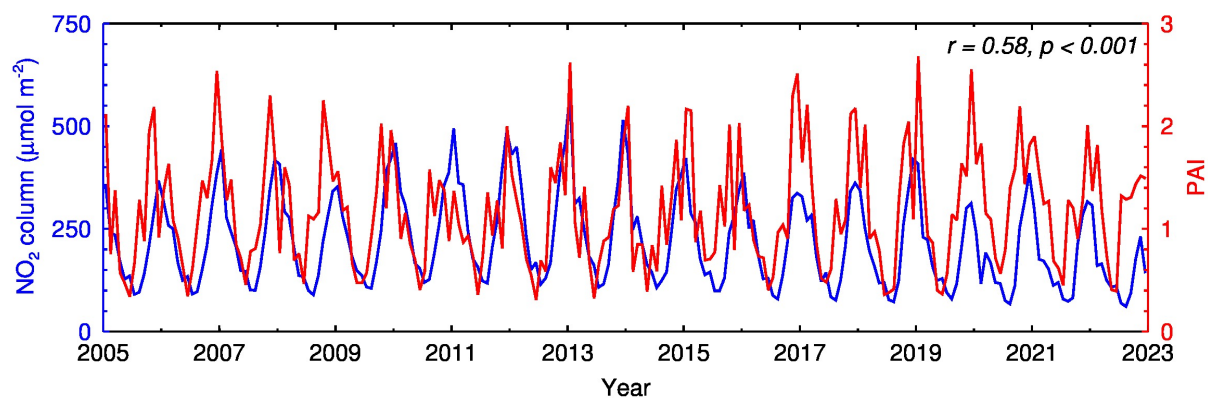


**Figure S2.** Linkage between NO<sub>2</sub> column and PAI. Long-term (2005-2022) monthly NO<sub>2</sub> column is generally connected to the PAI ( $r = 0.58$ , confidence level exceeding 99.9%) over North China, but there are noticeable discrepancies in the timings of the sub-peaks between them.

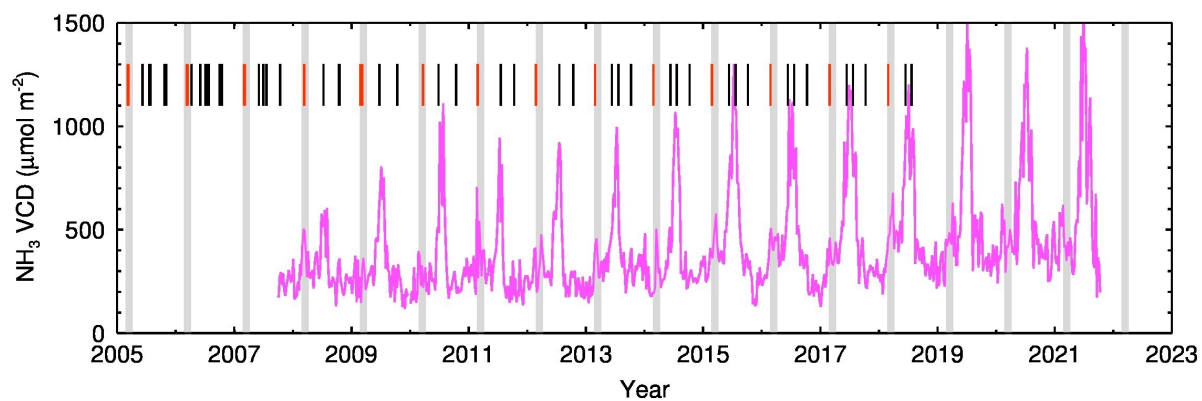


**Figure S3.** NH<sub>3</sub> column in March over North China. Long-term variation of seven-day mean tropospheric NH<sub>3</sub> column retrieved by IASI during the past two decades (2007-2022). The intersections of the gray bars and the pink lines, and the short bars are defined the same as Figure 1a.

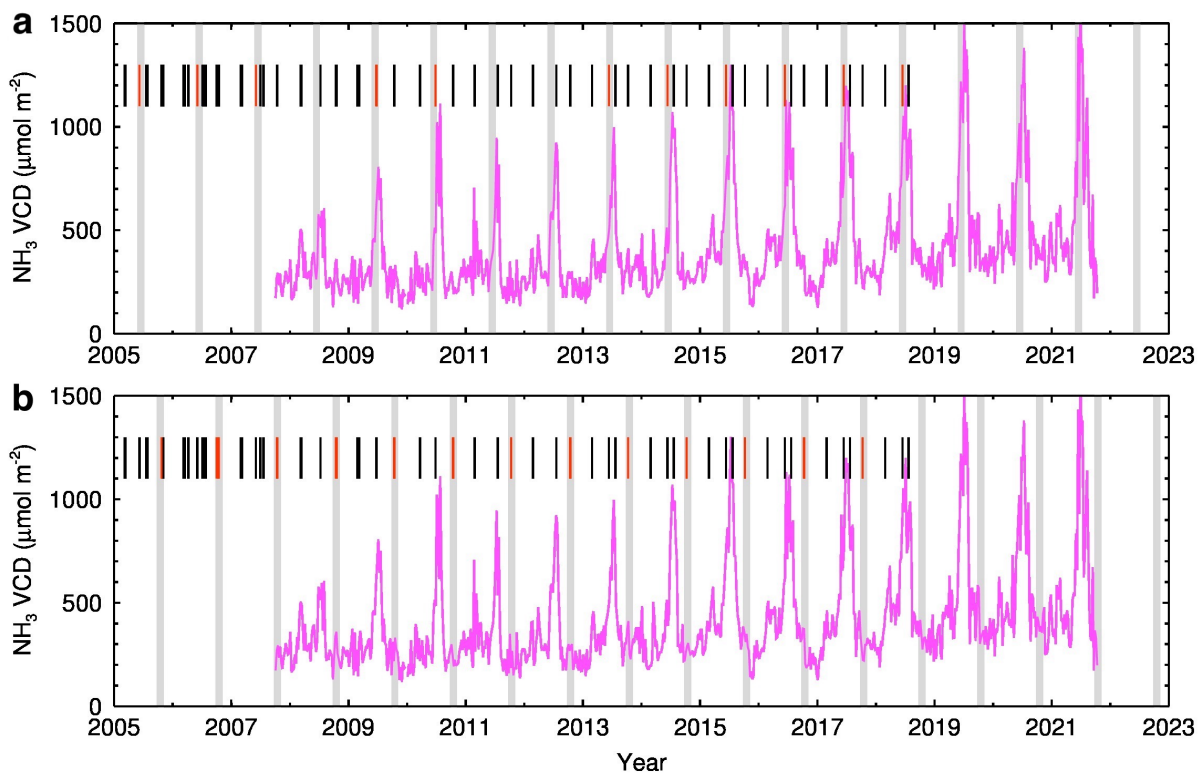


**Figure S4.** Other sub-peaks of NH<sub>3</sub> column. **(a and b)** Satellite-retrieved other pulses of NH<sub>3</sub> column in June and October, respectively. Intersections of the gray bars and the green lines, and the short bars are similar to those in Supplementary Figure 4.

## References

Feng, T., Zhao, S., Hu, B., Bei, N., Zhang, X., Wu, J., Li, X., Liu, L., Wang, R., Tie, X. and Li, G.: Assessment of Atmospheric Oxidizing Capacity Over the Beijing-Tianjin-Hebei (BTH) Area, China, *J. Geophys. Res. Atmos.*, 126(7), e2020JD033834, doi:10.1029/2020JD033834, 2021.

Huang, Q., Cai, X., Song, Y. and Zhu, T.: Air stagnation in China (1985-2014): Climatological mean features and trends, *Atmos. Chem. Phys.*, 17(12), 7793–7805, doi:10.5194/acp-17-7793-2017, 2017.

Korshover, J. and Angell, J. K.: A Review of Air-Stagnation Cases in the Eastern United States During 1981 - Annual Summary, *Mon. Weather Rev.*, 110(10), 1515–1518, doi:10.1175/1520-0493(1982)110<1515:AROASC>2.0.CO;2, 2000.

Su, T., Li, Z. and Kahn, R.: Relationships between the planetary boundary layer height and surface pollutants derived from lidar observations over China: regional pattern and influencing factors, *Atmos. Chem. Phys.*, 18(21), 15921–15935, doi:10.5194/acp-18-15921-2018, 2018.

Willmott, C. J.: On the Validation of Models, *Physical Geography*, 2(2), 184–194, doi:10.1080/02723646.1981.10642213, 1981.